International Journal of Scientific & Engineering Research, Volume 9, Issue 10, October-2018
ISSN 2229-5518

Engine Exhaust System Development & Optimization for FSAE Vehicle

Vasudev Gupta

Abstract - This paper focuses on ways in which the capabilities of an exhaust system are exploited in improving engine performance of an FSAE vehicle. The exhaust system specifically designed for the engine 2008 Honda CBR 600RR PC40, utilizes literatures on pressure wave propagation in ducts, reflection and transmission of incident pressure wave due to area discontinuity and impedance mismatch and driving point impedance of finite ducts, taking into account sensitive parameters such as temperature gradients which influence speed of propagation of wave and gas momentum variation, in order to determine the optimum dimensions of each exhaust system component, along with engine noise reduction without generation of back-pressure. Ricardo's one-dimensional engine simulation software – WAVE has been used to simulate and understand the sensitivities of various exhaust components on volumetric efficiency, exhaust gas scavenging efficiency and overall engine performance, to analyze the effect of exhaust gas flow through the combustion chamber and exhaust manifold. Moreover, meshing three-dimensional CAD parts and importing to WaveBuild workbench has been accomplished by WaveMesher, while Acoustic Acquisitions in WavePost has been used for engine acoustic simulations. Testing and validation of proposed methodology and design optimization techniques will be performed.

Index Terms – Acoustic Waves, Exhaust System, FSAE, Motorsports, Optimization, Powertrain Development, Ricardo Wave

1 Introduction

As thought by many, the exhaust manifold is not only utilized in directing exhaust gases post combustion but is much more potent in influencing the engine performance, in terms of, volumetric efficiency, exhaust residual, scavenging efficiency, and thereby augmenting engine power and torque characteristics. The primary goal of the exhaust manifold design proposed in this paper is to create a flatter engine torque curve, without lowering the peak torque magnitude, throughout the higher rpm, mainly from 7000-rpm; which has been established to maintain linear power delivery and predictable drivability while operating under this range. The Formula Student (or FS) engineering competitions, organized by the Formula Student of Automotive Engineers (or FSAE) is at the acme of engineering competitions conducted all around the world, and challenges the students towards innovative thinking, apart from having profound knowledge, skill and thinking capability to solve complex engineering problems. The competition involves both dynamic and static events, judging the teams and their vehicles for their knowledge, concept and design understanding, capabilities of implementing the literature onto their vehicle, design presentation and to achieve all these under low expenditures. The dynamic events include Acceleration, Autocross, Skid pad, Endurance and Efficiency; The design concept is targeted towards achieving highest in the Acceleration and Autocross category. The data acquired from various sensors on previous vehicles run under these events helped us to understand the vehicle state and establish the average engine rpm under which the vehicle operates, which was above the 7000-rpm region. A flatter torque and linear power curve has been achieved through careful design and simulation of the exhaust manifold.

The inline-4 engine used is normally categorized as a four-cycle unit. This may be true for passenger or street vehicle engines but is far from the case of a high-performance engine, comprising of a specific well-developed exhaust system, fine-tuned with valve operation and piston dynamics and can be said to have a fifth cycle added. With a tuned-length exhaust manifold, the negative pressure wave travelling back from the area discontinuity, produced by the collector, towards the exhaust port scavenges the remaining exhaust gases out of the combustion chamber, making possible higher volumetric efficiency, lower exhaust residual and greater power. The comparison between the piston's suction on the intake compared with the exhausts indicates the potential in exhaust tuning.

International Journal of Scientific & Engineering Research, Volume 9, Issue 10, October-2018
ISSN 2229-5518

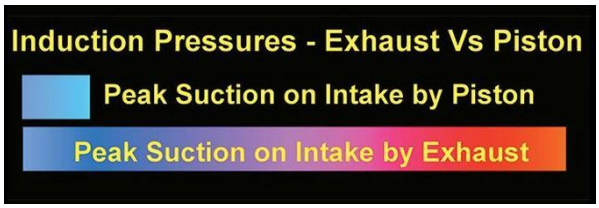

Not only is scavenging a benefit, the increased port velocity of incoming air due to suction by piston also allows for greater volume to be filled into the cylinder, and when fine-tuned with the intake manifold, the increased port velocity drives the cylinder filling above atmospheric pressure just prior to the point of intake valve closure. Compared with intake, exhaust tuning is far more potent and can operate over a much wider rpm band. [1]

To understand the effect of different iterations of the exhaust system on the engine, along with the extent of tuning, a theoretical engine model must be made to help in quick analysis and post processing, which is described in the next section.

- *Vasudev Gupta is currently pursuing bachelor's degree program in Automobile Engineering in Manipal Institute of Technology, Manipal, India. PH-9717210171. E-mail: guptavasudev37@gmail.com*

2 Development Of A Theoretcal Engine Model on RICARDO Wave

The exhaust system, having strong influence on engine performance, requires prerequisite data and understanding of the engine, such as firing order, opening and closing of valves and port geometries, intake and exhaust cam lobe profile, combustion chamber geometry; all of which were utilized to create a theoretical engine model on RICARDO's one-dimensional engine simulation software WAVE.

08 Honda CBR600RR Engine Specifications	
Displacement:	599.00 ccm (36.55 cubic inches)
Engine type:	In-line four, four-stroke
Compression Ratio:	12.0:1
Bore x stroke:	67.0 x 42.5 mm (2.6 x 1.7 inches)
No. of Valves:	4
Fuel system:	Injection. Dual Stage Fuel Injection
Intake Valves:	Opens - 21 deg bTDC
	Closes - 44 deg aBDC
Exhaust Valves:	Opens - 40 deg bBDC
	Closes - 5 deg aTDC
Valve control:	Double Overhead Cams/Twin Cam (DOHC)

To acquire the cam lobe profiles, the cam shafts were 3D scanned and verified using measurements done by dial indicator and valve models were created for both, intake and exhaust cams and the profiles are as shown below:

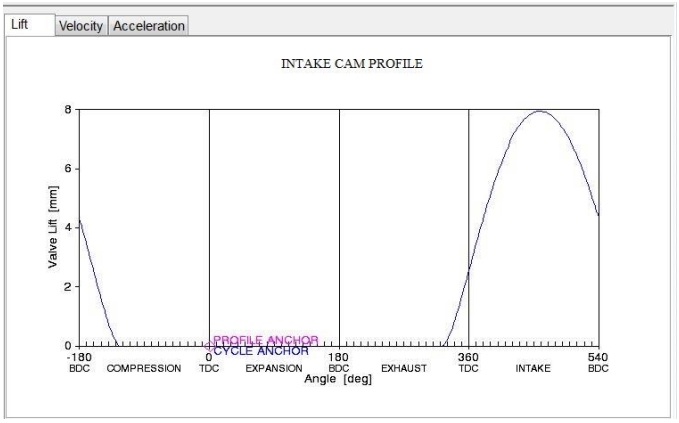

Fig 2.1 (i)

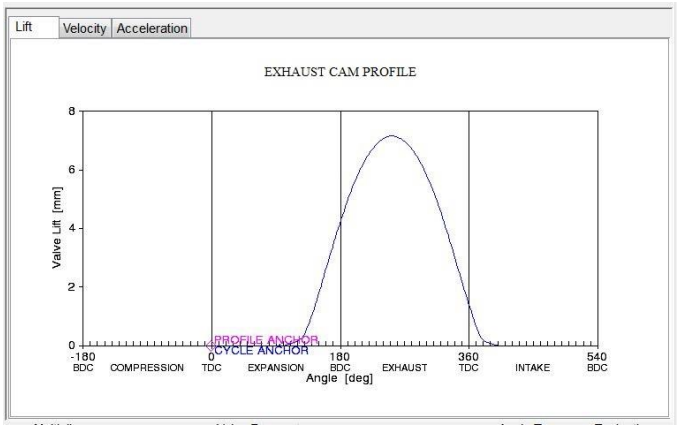

Fig 2.1 (ii)

International Journal of Scientific & Engineering Research, Volume 9, Issue 10, October-2018
ISSN 2229-5518

The Engine General Panel requires the Chen-Flynn Coefficients for calculation of frictional mean effective pressure (fmep) of the engine, and the data for Wiebe Combustion Model to evaluate the combustion characteristics at a constant rpm, which couldn't be determined without experimental testing. These were initially taken to be default values from WAVE's tutorial and were determined at a later stage after creating a working engine model. The intake and exhaust used were constructed using ducts and orifices from the RICARDO library (Fig.2.2).

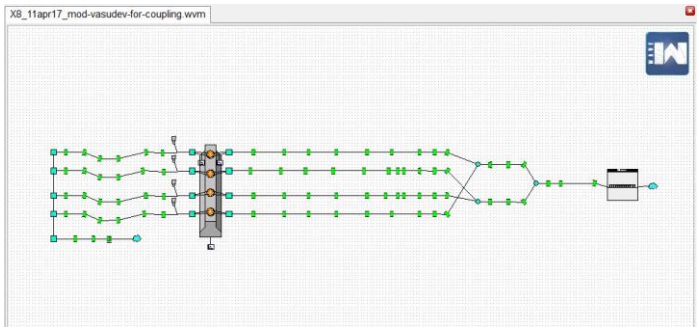

Fig 2.2

The torque and power curves obtained through dynamometer testing were compared to the base model established above, were this comparison indicated large deviation from the actual curve caused by the inaccuracies of the engine peripherals made using ducts, orifices and Y-junctions. These were replaced by importing CAD files to RICARDO's WaveMesher (Fig2.3, i & ii), which facilitated their meshing and introduction to the engine model (Fig2.4). As predicted, the substitution to meshed three-dimensional CAD components indicated closer resemblance to the engine power characteristics (Fig2.5).

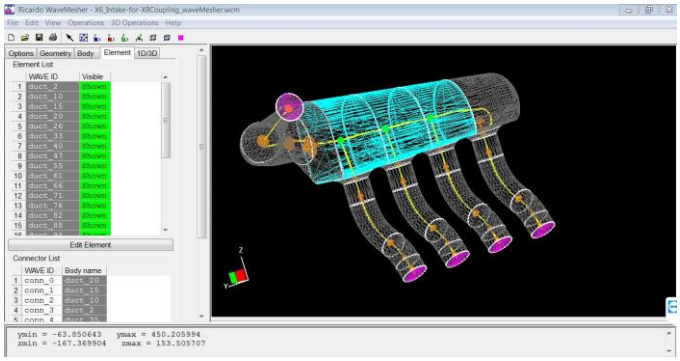

Fig 2.3 (i)

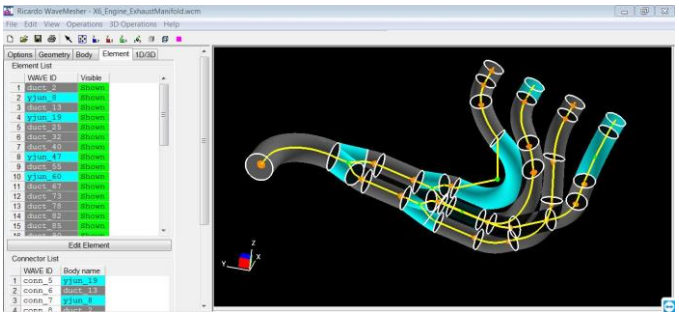

Fig 2.3 (ii)

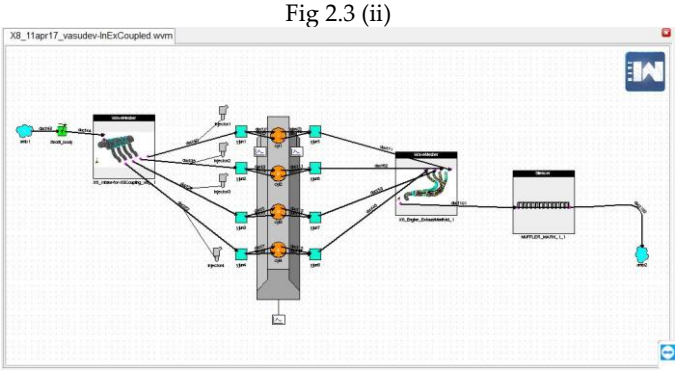

Fig 2.4

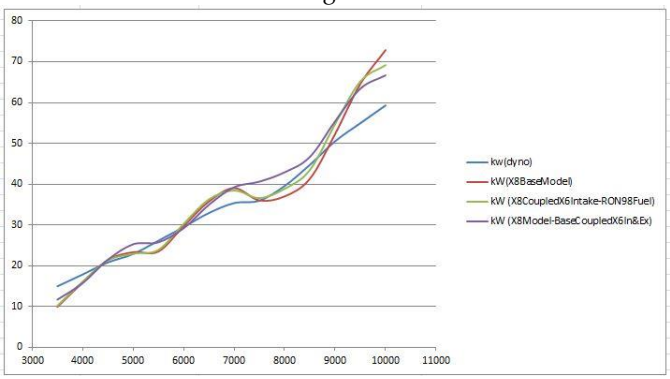

Fig 2.5

The only factor leading to deviation from actual engine performance curves were Chen-Flynn coefficients for the friction model and Wiebe combustion model data. These were corrected through trial and error process, referencing studies done by Emiliano Pipitone on evaluation of a simple friction model for a S.I. engine [2], P M V Subbarao on Nature of Heat Release Rate in an Engine [3] and Willard. W. Pulkrabeck [4]. Fig2.6 (i & ii) shows the final friction model and Wiebe combustion model respectively, while Fig2.7 (i & ii) indicates the final brake horsepower curve from the theoretical engine model compared with actual curve obtained through testing. **Close resemblance of power characteristics of theoretical model with actual setup averred its reliability and efficacy of further simulations performed using it as a platform.**

International Journal of Scientific & Engineering Research, Volume 9, Issue 10, October-2018
ISSN 2229-5518

Fig2.6 (i)

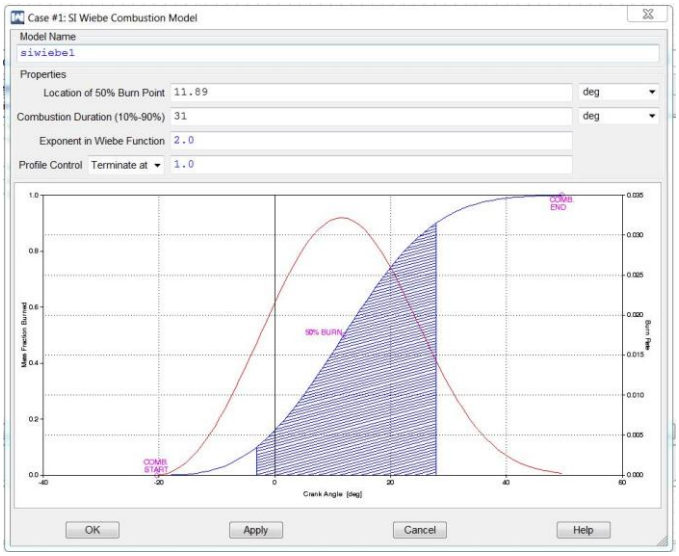

Fig2.6 (ii)

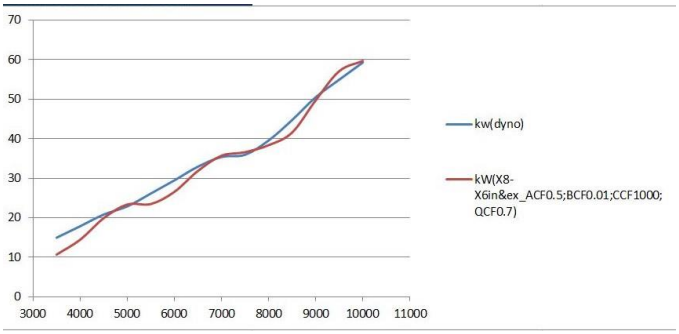

Fig 2.7 (i)

rpm	kw(dyno)	
3500	14.96823273	10.68109989
4000	17.85612545	14.44287014
4500	20.81180909	19.89838028
5000	22.87943182	23.36227036
5500	26.13339545	23.47707939
6000	29.46192909	26.55846024
6500	32.93282364	31.85508919
7000	35.36651727	35.7060585
7500	35.94274	36.59553146
8000	39.55599545	38.36661911
8500	44.73522091	41.57234955
9000	50.51100636	49.71746826
9500	54.94453182	57.09452057
10000	59.30348727	59.7036705

Fig 2.7 (ii)

3 Exhaust Manifold Design Considerations

In this paper mainly two broad categories of exhaust manifold configurations are analyzed, known to be the 4-to-1 (right – Fig3.1) and 4-to-2-to-1 or the Tri-Y headers. (left - Fig4.1).

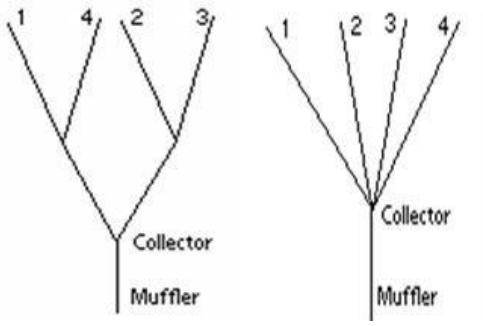

The former exhaust manifold design, a 4-2-1 configuration was changed to 4-1 to evaluate the influence on the power and torque curve of the engine, and the CAD of which is shown in (Fig3.2). The 4-1 configuration, lacking the secondary header element, yields peak torque earlier in the RPM range compared to the 4-2-1, while a linear power curve in obtained in the latter case (Fig3.3 (i & ii)). This is because secondary headers create a higher power band due to tunability at multiple rpms.

International Journal of Scientific & Engineering Research, Volume 9, Issue 10, October-2018
ISSN 2229-5518

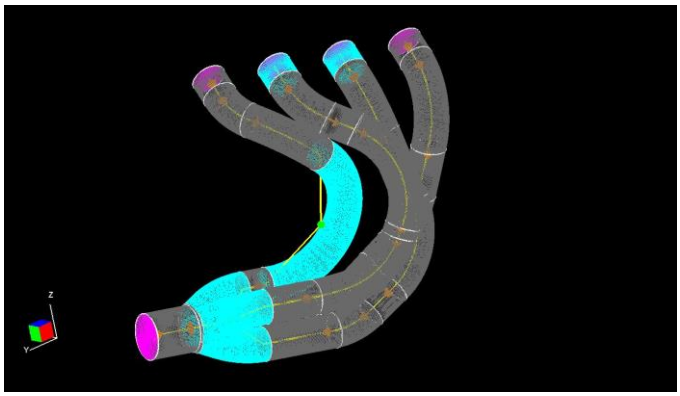

Fig 3.2

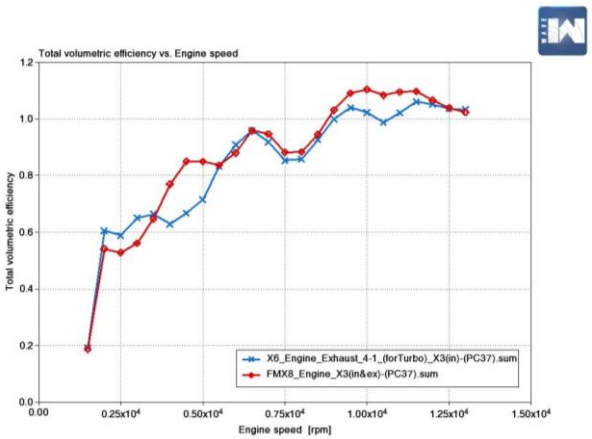

Fig 3.3(i)

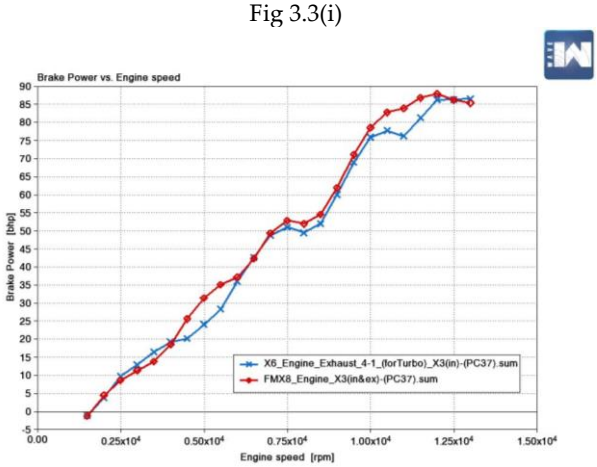

Fig 3.3(ii)

4 Primary Header Length & Diameter Determnation

4.1 Primary Header Length

The opening of the exhaust valve post combustion creates a pressure wave at the exhaust valve which propagates through the exhaust port and into the primary header, at the speed of sound at that pressure and temperature, till it encounters an area discontinuity or a boundary after which the impedance of the medium changes. As this happens, some energy is reflected while the remaining is transmitted in the direction of incident. The frequencies of the incident, reflected and transmitted wave are assumed to be constant, based on linear acoustics, for simple evaluation. This impedance mismatch is encountered midway of the primary collector, and as the collector impedance is lesser then that of primary header (due to greater area, hence lesser density), the positive pressure wave incident, changes phase by 180 degrees and is reflected as a negative pressure wave. This happens because, as it travels into a greater area, its pressure falls quickly and because of its momentum to travel away from the primary header end, it creates a little suction, i.e. the gas behind it is sucked out, and hence a below atmospheric (negative) pressure wave travels back to the exhaust port [5], [6] and [7]. The length of the primary header is tuned with the intake and exhaust valve lift profiles for the reflected wave to reach the exhaust port at the time when the intake valve is 1mm (0.05") open. The exhaust valve takes 54 degrees to open from 0 to 0.05" (1mm) lift, while 0.05" being 40 degrees bBDC. The return of negative pressure wave has been predicted to be around 21 deg bTDC, at the location where the intake valve is 0.05" (1mm) open (Fig2.1(i & ii)). This location with respect to the exhaust valve is closer to its maximum lift. Due to upward momentum of piston, the outrush of exhaust combined with huge pressure differential due to negative pulse, promotes great scavenging phenomenon. This means the cylinder scavenging pulse should return after 253 deg of cam revolution. The real time taken for this pulse to return to valve depends on tuned engine rpm.

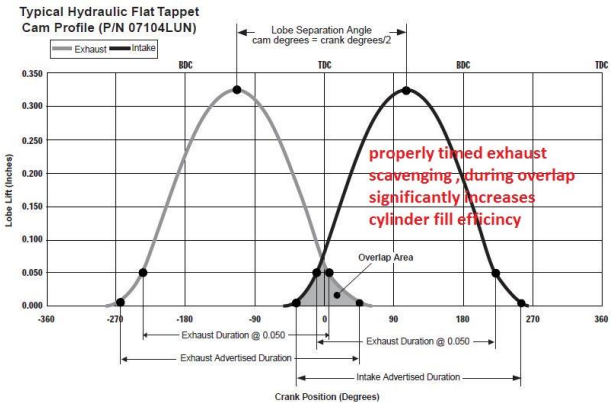

Fig 4.1

International Journal of Scientific & Engineering Research, Volume 9, Issue 10, October-2018
ISSN 2229-5518

The temperature of exhaust gas at exhaust port obtained from this theoretical model came out to be around 1200K at the desired rpm, which was also verified through an EGT sensor mounted near the exhaust port on former exhaust system (Fig4.2). At this temperature, sound speed was calculated to be 681 m/s, considering isentropic wave propagation (Fig 4.3).

Gas Constant of Exhaust Gases (J/Kg.K):	287	
Exhaust Port Average Temperature (K):	1200	SONIC VELOCITY
Specific Heat Ratio:	1.35	
Sonic Velocity at above Temperature (m/s):	681.865089	

Fig 4.3

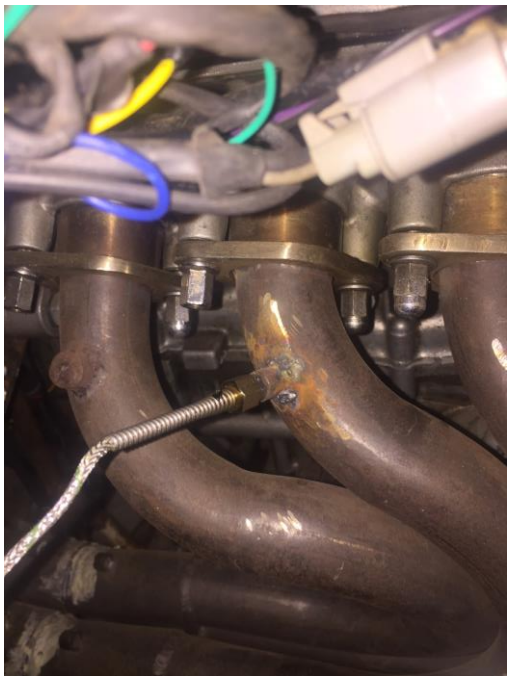

Fig 4.2

The length of the primary headers was calculated at increments of 500 rpm and at different harmonics, where real time required for 1-degree cam rotation was calculated for each step and was multiplied by 253, to obtain real time required for 253 degrees of exhaust cam rotation, which must be the time in which the negative pressure wave is predicted to reach exhaust port to promote scavenging and enhance cylinder filling (Fig 4.4).

As the length increases, the pressure wave would reach the port later, hence improving volumetric efficiency at lower rpms, while decreasing primary length means to tune at higher rpms (Fig 4.5). Moreover, tuning at a higher harmonic means to obtain a smaller length hence improving packaging, but is understood by the fact that the pressure wave would oscillate more, hence losing its energy at every reflection. This would eventually make the pressure to reach nearly atmospheric and no significant effect would be observed.

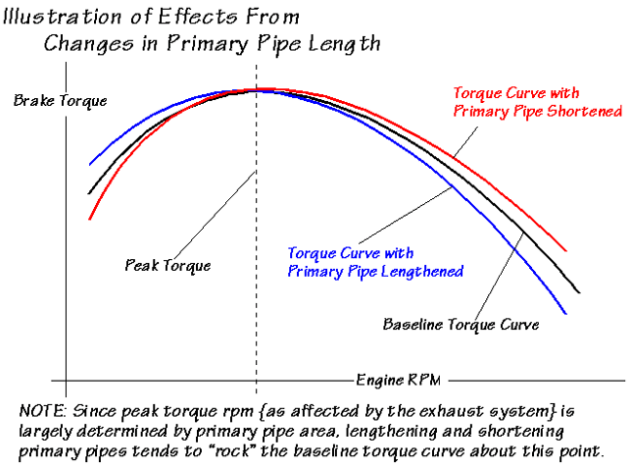

Fig 4.5

To determine the optimum primary header length to make the reflected wave incident on the exhaust valve at time of intake valve opening at 10,000 rpm, the RICARDO engine model was updated with the new intake manifold (Fig4.6) and ducts and Y-junctions resembling a 4-2-1 exhaust manifold, with a variable defined for primary length (Fig4.7). A plot for pressure at the exhaust port was studied to verify and fine-tune the length of primary header (Fig4.8).

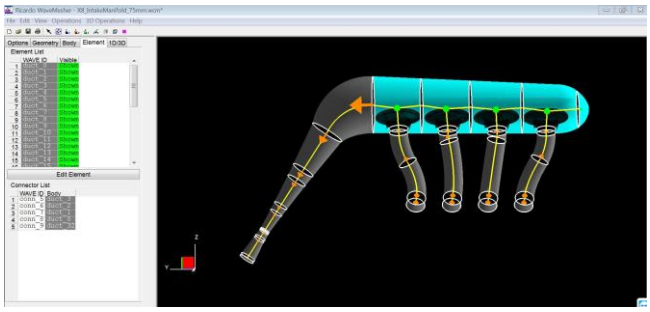

Fig 4.6

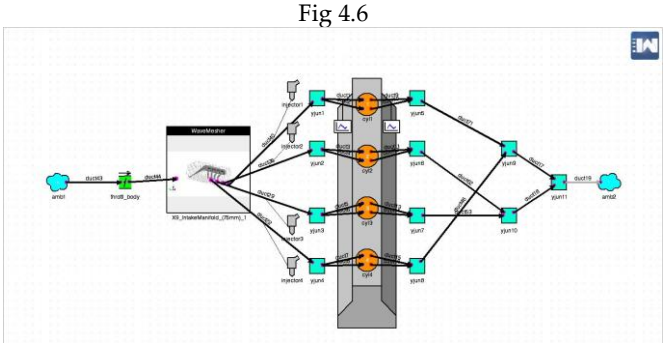

Fig 4.7

International Journal of Scientific & Engineering Research, Volume 9, Issue 10, October-2018
ISSN 2229-5518

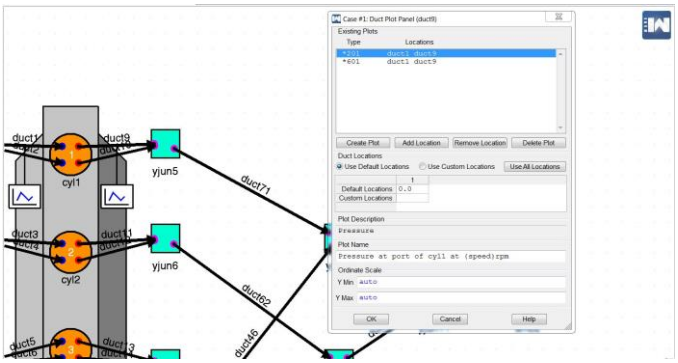

Fig 4.8

The primary length was varied from 200 to 350 mm and scavenging efficiency, volumetric efficiency and residual gas fraction plots was created to observe the effect of length variation. Also, the pressure amplitude of the wave incident on the exhaust port was also noted by plotting the pressure vs rpm curves, to determine the energy loss for every harmonic. These are shown in (Fig 4.9 (i, ii, iii & iv)) respectively, and resemble the variations predicted by theory. (Fig4.10) shows different port pressure plots for constant primary length and at different rpms.

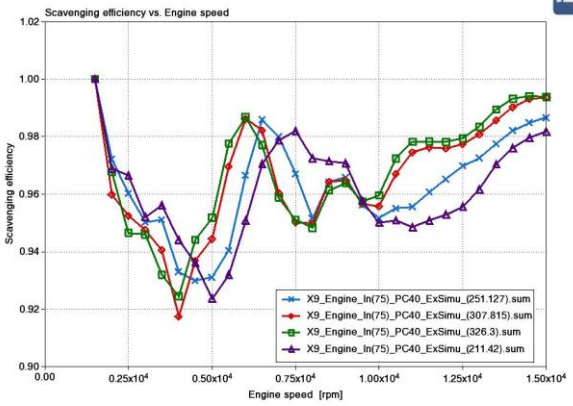

SCAVEF vs RPM - Fig 4.9 (i)

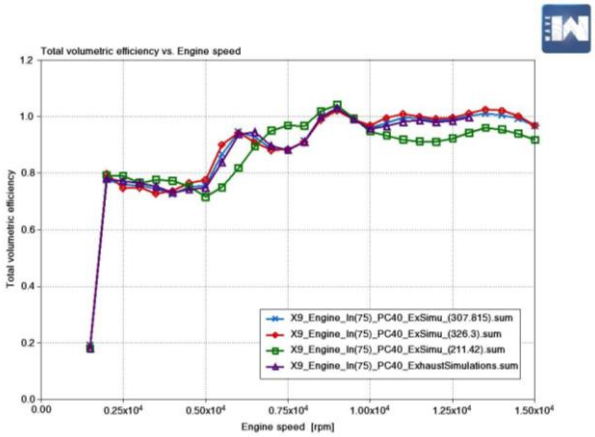

VOLEF vs RPM – Fig 4.9 (ii)

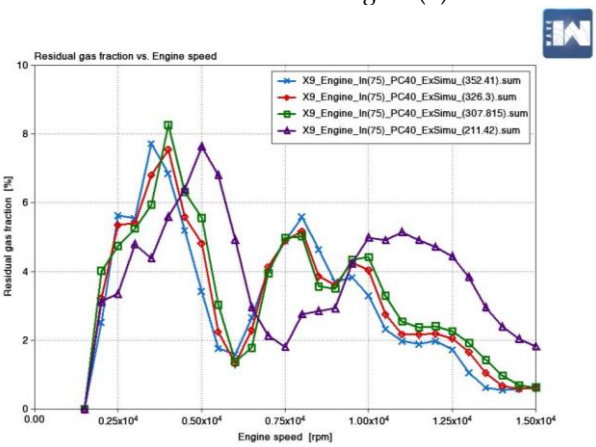

RES% vs RPM – Fig 4.9 (iii)

As calculated in using Microsoft excel (Fig4.4), the tuned length was determined to be 358.8mm at 10,000 rpm and at the exhaust temperature of 1200K, which was also verified by analyzing pressure vs rpm plot at exhaust port (Fig 4.11 (i &ii)).

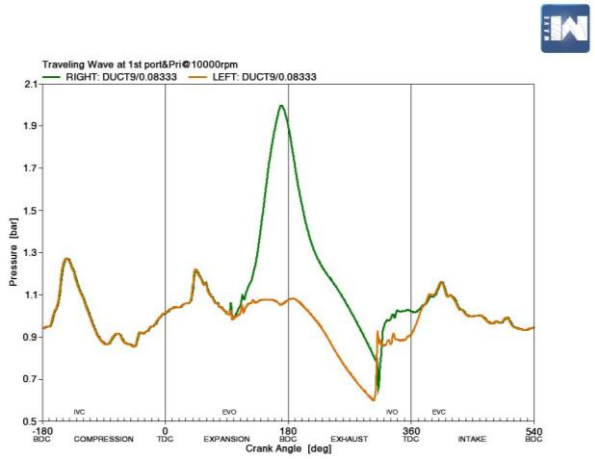

Fig 4.11 (i)

International Journal of Scientific & Engineering Research, Volume 9, Issue 10, October-2018
ISSN 2229-5518

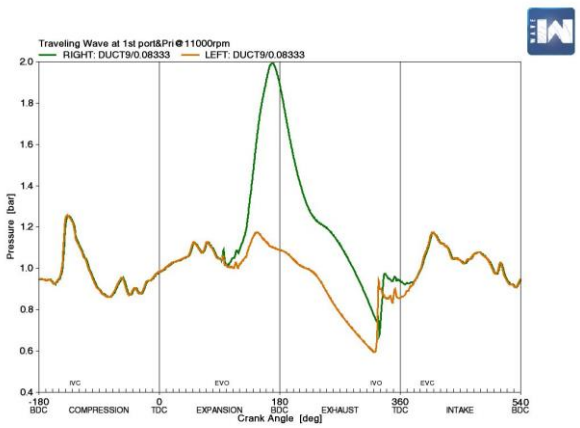

Fig 4.11 (ii)

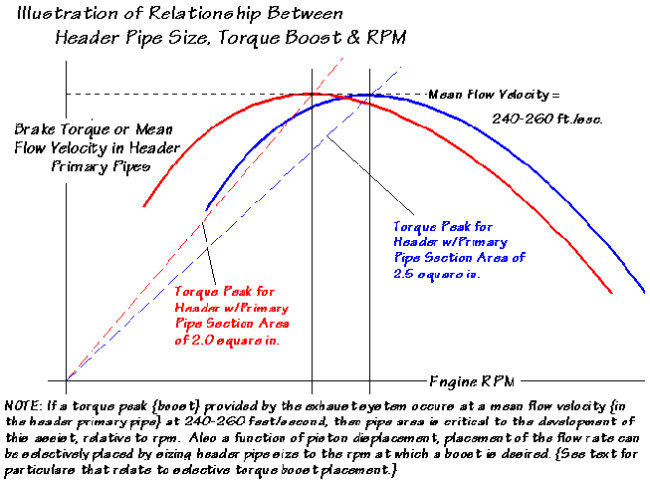

Fig 4.12

4.2 Primary Header Internal Diameter

The exhaust pipe internal diameter has a prominent role in extracting exhaust out of the cylinder and preventing reversion of exhaust into the intake manifold. This is achieved by inertial scavenging i.e. through the inertia of exhaust gases rushing out from the combustion chamber. This also forces fresh air/fuel charge into the engine. The smaller the pipe diameter is, the greater would be its velocity and hence inertia, but this would also restrict higher gas flow rate required at higher rpms. Moreover, designing an exhaust with bigger pipe diameters would lead to slower gas velocities. To determine the optimum internal diameter or area of exhaust piping, one must understand that engines are flow sensitive, not size sensitive, and calculation of pipe area based on flow rate of exhaust gas at peak valve lift and wide-open throttle required at the desired rpm is of prime importance. The primary pipe area determines the peak torque rpm, while varying the primary length rocks the curve at this peak rpm (Fig4.12).

Determination of optimal exhaust primary diameter is based on determining the exhaust gas flow rate at desired peak torque rpm. The mass of intake charge ingested by the engine is equal to mass of exhaust gas post combustion, but the volume of exhaust is much more than that of intake charge due to oxidation reaction of fuel and thermal expansion. For simpler calculation, an air-standard cycle with 100% volumetric and combustion efficiency had been assumed. As the stochiometric combustion of exhaust occurs, 1 mass of fuel (assumed to be octane – C_8H_8) and 14.7 by mass of air (with almost 21% oxygen) is converted to CO_2 and H_2O. Oxidation of octane generates 9 moles H_2 and 8 moles CO_2, with 12.5 moles of air used for 1 mole of octane. For gas volume purposes, the assumption has been taken that equal mass of gas produces equal volume. This process yields the resulting post combustion volume of exhaust gas. From the ideal gas law, we know that the increase in volume of the exhaust gas will be proportional to the increase in absolute temperature, and the ratio of exhaust volume to intake volume will be equal to ratio of their absolute temperatures, revealing the increasing of volume due to thermal expansion [4]. The below mentioned formula derived based upon similar studies is used for calculating primary pipe diameter (with all dimensions in inches):

$$\text{Primary Pipe Area} = \frac{(\text{peak torque rpm x displacement of each cylinder})}{88{,}200}.$$

International Journal of Scientific & Engineering Research, Volume 9, Issue 10, October-2018
ISSN 2229-5518

Moreover, the market availability of pipe diameters was taken into consideration, and RICARDO engine model's exhaust system was updated with primary diameters of 31.75 (red), 35.1 (green) and 38.1 (blue) mm for a constant primary header length and the plots generated are presented below (Fig 4.13 (i, ii & iii)):

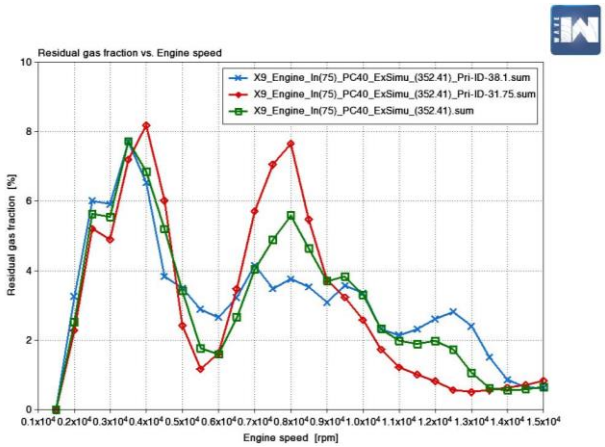

Residual gas fraction – Fig 4.13 (i)

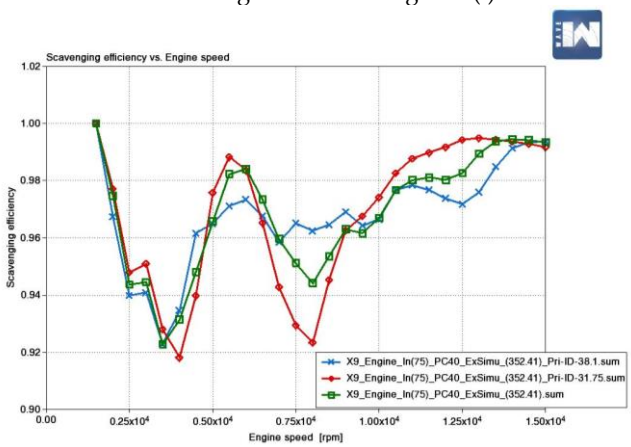

Scavenging Efficiency – Fig 4.13 (ii)

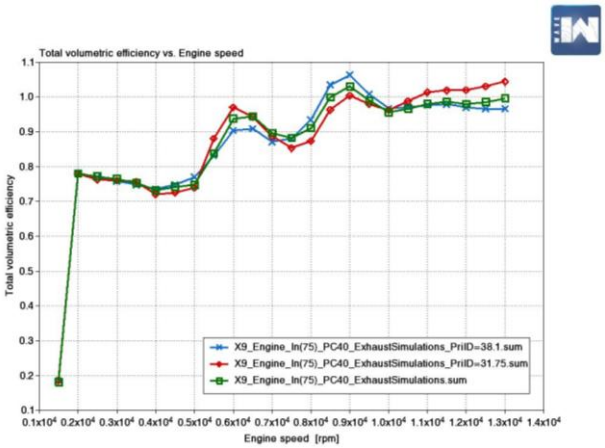

Volumetric Efficiency – Fig 4.13 (iii)

Increasing the operating range of the engine means that it must be able to pump exhaust gas out without experiencing any back pressure. To allow the engine to do so, the primary pipe diameter was calculated to be 31.75mm tuned at 12,000 rpm. The first design of side-exit exhaust with only primary headers, with calculated length and pipe diameter, was created on Catia V5 (Fig4.14), with respect to the engine, chassis and other surrounding components, meshed and imported to the WaveBuild canvas of the engine model on RICARDO, replacing the test exhaust made using ducts and orifices.

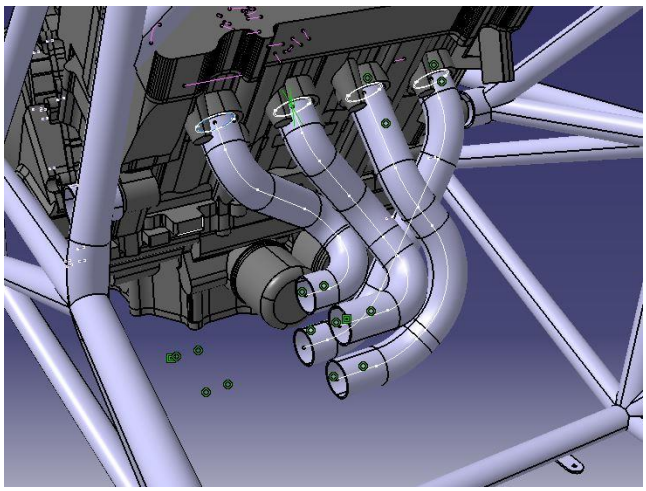

Primary Headers – Fig 4.14

A higher bend radius meant higher flow capabilities with lesser losses due to flow separation, eddy formation and viscous energy dissipation. Moreover, manufacturing higher radius bends is also easier, although these create packaging difficulties. A side-exit exhaust generates difficulties in equating all header lengths, but to compromise between optimization and packaging constraints, the design was made for the lengths to be under 15% deviation from the optimum value. Pipe bends' market availability was considered and exhaust system with 2D bends (Bend Radius = 2 x Pipe OD) was designed. (Fig4.15) shows the pressure plot at 1st exhaust port indicating that the negative pressure pulse reaches just before opening of intake valve at 10,000 rpm while just after its opening at 12,000k rpm. Although this iteration showed close to optimum results, more designs were made to improve fixture manufacturing and packaging, though they proved to be futile.

International Journal of Scientific & Engineering Research, Volume 9, Issue 10, October-2018
ISSN 2229-5518

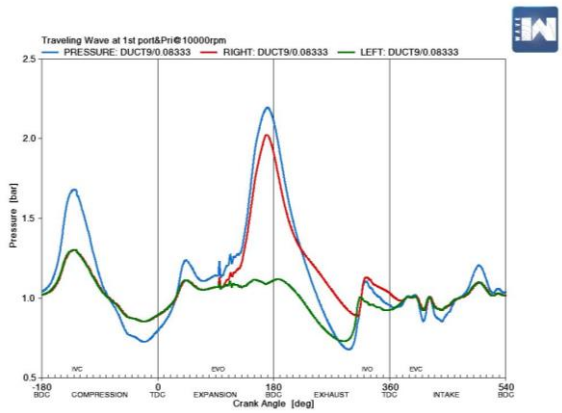

Fig 4.15

5 Primary Collector

The collector has the task to cumulate exhaust gases entering from the primary headers pairs that are separated as far apart as possible in the firing order providing an increase in volume for the combined gas to continue flowing. As the firing order of the engine used is 1-2-4-3, cylinders 1-4 and 2-3 are paired together into one primary collector. The boundary of increase in area or volume in the collector creates an impedance mismatch, making the incident wave to reflect and transmit at this boundary. The reflected wave is used for tuning primary lengths, while the transmitted wave is put to use when tuning secondary headers. The availability of secondary headers helps in fine tuning the exhaust system to work at the desired rpm range, providing a broader-range performance [8,9]. As the pressure wave enters the primary collector before reflection, some length of the collector is added to the overall length of primary header, hence reduction in primary header length must be done to compensate for this increase.

Moreover, the collector entrance angle (or cone angle) must be kept as small as possible in order to assist gases in changing directions and maintaining streamlined flow for improved cylinder scavenging which is why most high-performance collectors are having 10-20^{o} entrance angle, with 15^{o} being considered optimal.

5.1 Best-fit Collector for High Performance Engines

Two categories of collectors were studied, namely parallel and merge collectors. Having the same entry angle of primary pipes into the collector, the parallel collectors offers a sudden increase in area causing adverse pressure gradient for the gases leading to their separation from boundary layer and can sometimes create flow reversal at low rpms. This phenomenon influences the gas entering from the oppositely paired header into the collector restricting its flow and causes mixing. It also diminishes the influence of header tuning while making the system unpredictable and insensitive with generation of back pressure.

Conversely, a merge collector has an entrance cone (or goilet) which is the outcome of the primary pipes converging, creating more smoother transition into the higher cross-section area region of the collector [1,7,8]. (Fig5.1(i & ii)) shows 4-1 parallel and merge collector designs:

Parallel Collector – Fig 5.1 (i)

Merge Collectors – Fig 5.1 (ii)

The collector design has a great impact on exhaust gas flow and header tuning, which is why a merge collector of 15^{o} entrance angle was designed.

The collector inlet center separation must be small enough to allow for steady transition and to occupy less space. Moreover, difficulty in assembly and welding arises at the mating interface of the two converging

International Journal of Scientific & Engineering Research, Volume 9, Issue 10, October-2018
ISSN 2229-5518

headers due to lesser gap available for the welding torch. For this reason, the separation between the outer surfaces of the inlet to collector was made to be a slightly higher than the welding torch width (20mm). The wall thickness being 1.5mm, the collector inlet separation was calculated to be 54.75mm for the primaries with outer diameter being 34.75mm (Fig5.2).

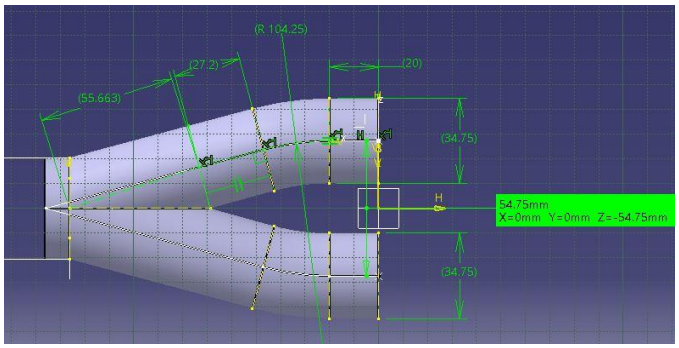

Fig 5.2

The change in the dynamic state of the incident wave due to its encounter with the impedance boundary at almost the mid region of the collector depends on the difference in characteristic impedance of the two mediums (Fig 5.3).

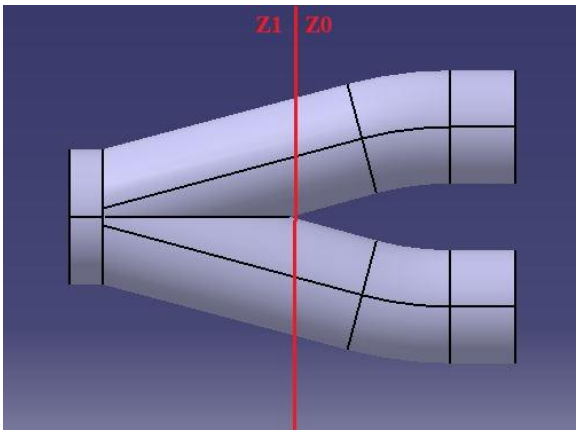

Fig 5.3

The characteristic impedance (Z) of a medium defines the response of that medium in its ability to propagate a pressure wave due to a forcing boundary condition i.e. how effectively the force can generate a given velocity of propagation and is the ratio of the complex pressure of that wave to corresponding complex velocity. It is also the product between the density of the medium and velocity of propagation (which is the sound speed). For the purpose of analysis, the system was assumed to be in the linear acoustic domain and was evaluated to determine the extent of reflection and transmission and its dependency on change in impedance. The reflection (R) and transmission coefficients (T) were defined as ratio between reflected and transmitted pressure to incident pressure respectively, and were calculated to be:

$$\text{Reflection Coeff. (R)} = \frac{(Z1 - Z0)}{(Z1 + Z0)}$$

$$\text{Transmission Coeff. (T)} = \frac{2\,Z1}{(Z1 + Z0)}$$

Where, Z_0 and Z_1 defines the characteristic impedance of the two medias.

As Z is the product of media density and sound speed, the density of volume in the collector is lesser than that in the header pipe, making $Z_1 < Z_0$. This makes the reflection coefficient negative, meaning that the reflected wave is 180° out of phase with the incident wave i.e. a negative pressure wave created from an incident positive pressure wave. The amplitude of this reflected wave depends on the difference between the impedances of the medias, and hence the impedance of collector must be made as small to reflect high negative amplitude pressure wave directed to the exhaust port for improved scavenging. However, that compromises the value of transmission coefficient and losing the advantage of the secondary header tuning.

6 Secondary Header Length & Diameter Determnation

6.1 Secondary Header Internal Diameter

The exit diameter of the collector or the diameter of the secondary header plays an important role in defining the density and hence the characteristic impedance of the primary collector, which was analyzed by creating different collector models with 15° entrance angle, 54.75mm inlet center distance and available pipe diameters of 38.1, 41.45 and 44.45mm, meshed and added to the engine model downstream of the primary exhaust model and simulated on WAVE; (Fig 6.1 (i, ii, iii & iv):

International Journal of Scientific & Engineering Research, Volume 9, Issue 10, October-2018
ISSN 2229-5518

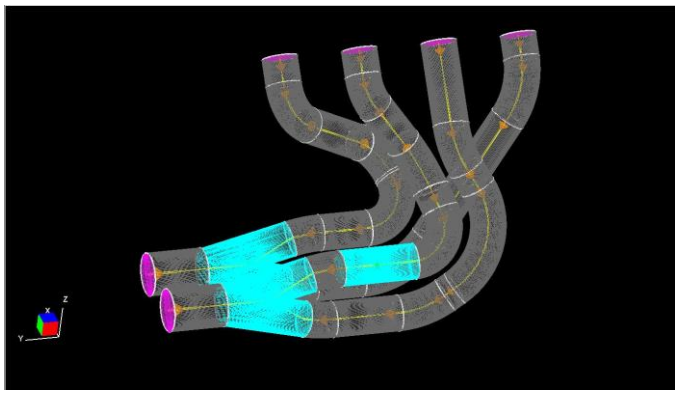

Fig 6.1 (i)

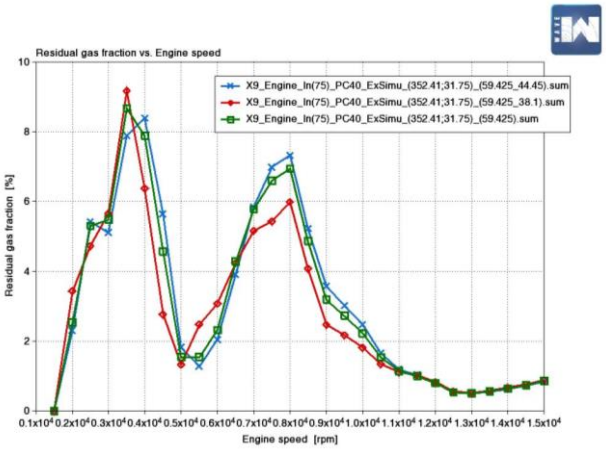

Residual gas fraction – Fig 6.1 (iv)

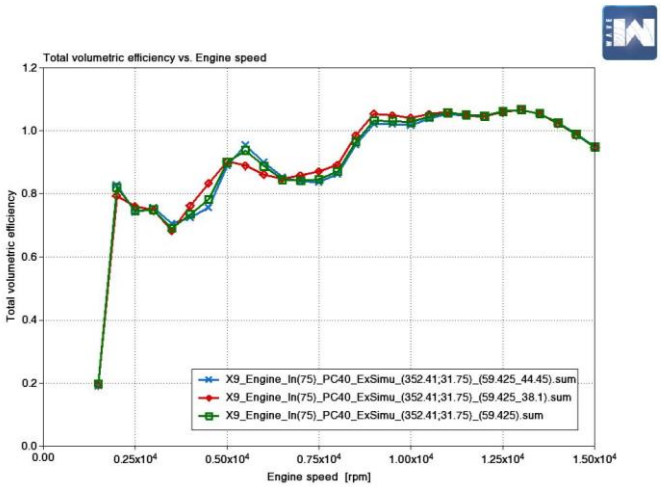

Total Volumetric Efficiency – Fig 6.1 (ii)

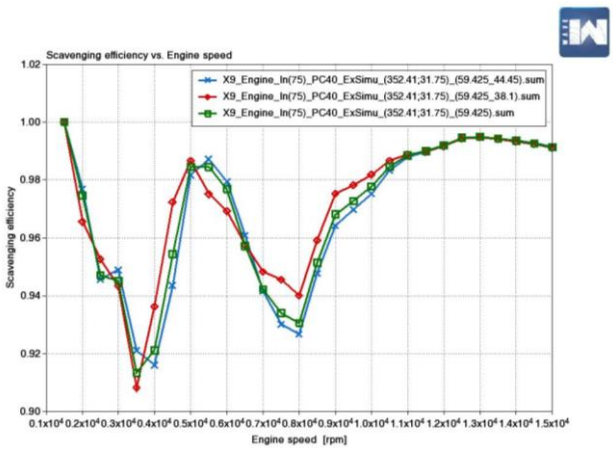

Scavenging Efficiency – Fig 6.1 (iii)

Based on the above engine performance plots, the secondary header diameter of 38.1mm was chosen, as this provided higher top-end volumetric efficiency, a flatter torque curve, greater exhaust scavenging and lower exhaust gas residual in the combustion chamber.

6.2 Secondary Hedaer Length

The tuning of the secondary header is different than the primary ones as, in this case the transmitted pressure wave from the primary collector must travel through the secondary header, reflect from the secondary collector and be incident on the primary collector impedance boundary in order to create a negative pressure or vacuum region to force pull more exhaust gas from the second primary header end of the pair. As the firing gap between these two paired headers is 360°, this meant that the reflected wave must reach after 360° of crank rotation back to primary collector. On this basis, the secondary header length was calculated and is present in the excel table (Fig 6.2).

Temperature at each exhaust component was determined through simulations on WAVE, and secondary inlet gas temperature of 900K was found, with a sound speed of approximately 590.5 m/s.

Using the calculated length, the exhaust manifold was modified with secondary headers, and the lengths were further tuned through trial and error using pressure plots at entry and exit of secondaries. 59.425mm and 118.85mm lengths, with a constant 15° entrance angle and 44.45mm outlet diameter for secondary collector, were obtained and verified to attain anti-resonance in the secondary headers (Fig 6.3 (i, ii & iii)). Exhaust residual curve was also studied to observe the effect on overall performance of exhaust system on cylinder scavenging (Fig 6.4).

International Journal of Scientific & Engineering Research, Volume 9, Issue 10, October-2018
ISSN 2229-5518

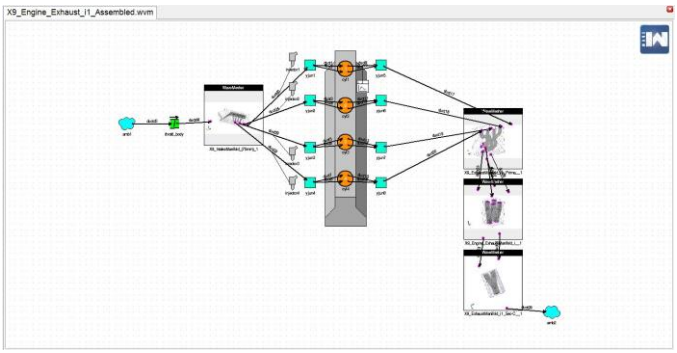

Engine model on WaveBuild with assembled exhaust components – Fig 6.3 (i)

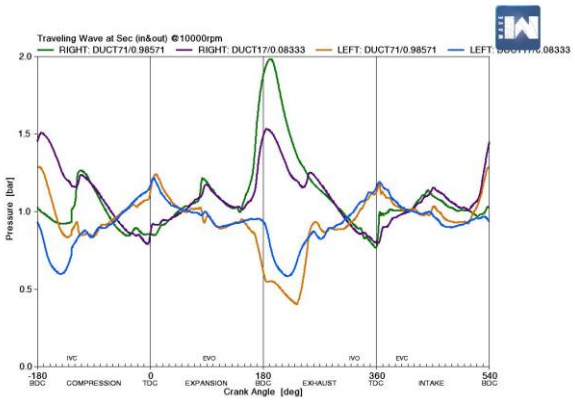

Pressure Plot for 59.4mm secondary – Fig 6.3 (ii)

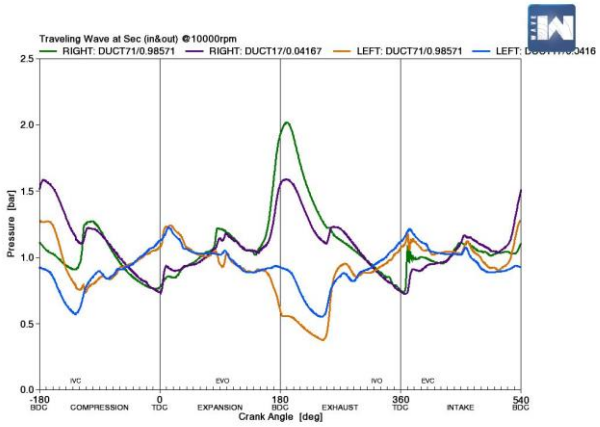

Pressure Plot for 118.85mm secondary – Fig 6.3 (iii)

Both lengths delivered the expected result of directing oppositely phased (negative) pressure wave at the inlet of the secondary pipe and creating anti-resonance to decrease the pressure in the pipe for improved exhaust gas scavenging.

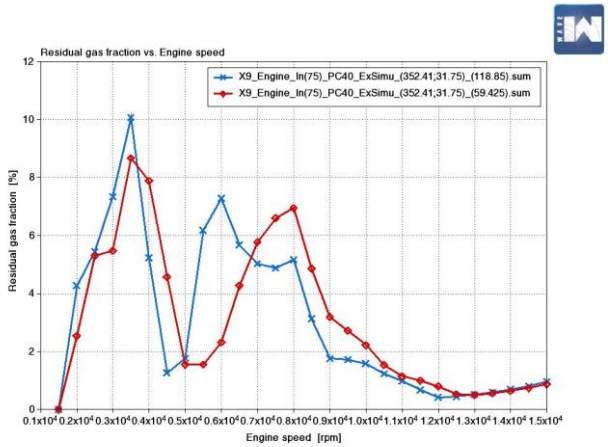

Residual gas plot comparing both secondary lengths - Fig 6.4

Exhaust residual gas fraction plot shown above indicated desired performance characteristics by 118.85mm secondary header at higher rpm engine operation (above 7k). The total length of 118.85mm is the combination of part of primary collector, secondary header length and part of secondary collector, as the transmission and reflection occur at boundaries of impedance mis-match mid-way between the collectors.
(Fig 6.5 (i & ii)) shows the rendered graphic of the exhaust manifold with the components and its routing with respect to the chassis and engine.

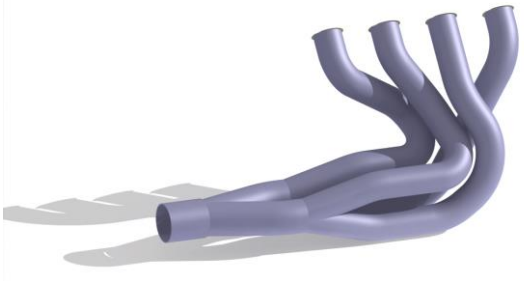

Fig 6.5 (i)

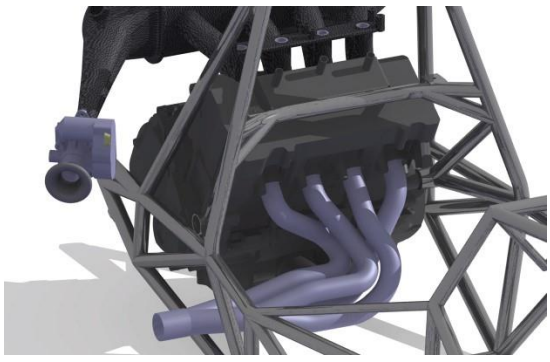

Fig 6.5 (ii)

International Journal of Scientific & Engineering Research, Volume 9, Issue 10, October-2018
ISSN 2229-5518

7 The Downpipe or Collector Extenstion

The downpipe or the collector extension, added downstream of the secondary collector, acts as another element which when tuned properly helps scavenge exhaust gas from the secondary headers, increasing and flattening mid-range torque, and making the engine to deliver a linear power output (Fig 7.1 (i & ii)).

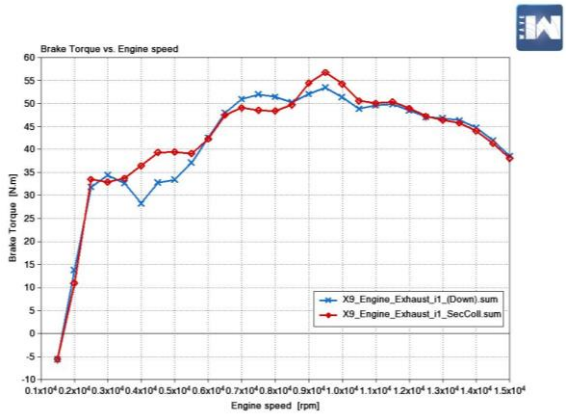

Flatter torque output achieved through collector extension - Fig 7.1 (i)

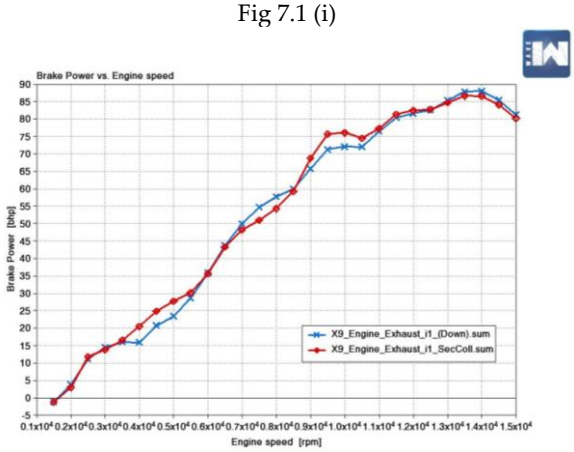

Linear engine power delivery achieved by adding collector extension – Fig 7.1 (ii)

Moreover, the downpipe also facilitates the assembly and mounting of the muffler, as it can be routed alongside the vehicle's side impact structure.

On similar basis of tuning the secondary headers, the reflected wave from the downpipe outlet must also reach the secondary collector after 360° of crank rotation, to draw exhaust gases from oppositely paired secondary header and boost scavenging. Various downpipe lengths were simulated to observe a phase difference of 180° between incident and reflected wave inside the downpipe, and the calculated length of 208.7mm (Fig 7.2) was optimized to 212.6mm, with the results shown in (Fig 7.3).

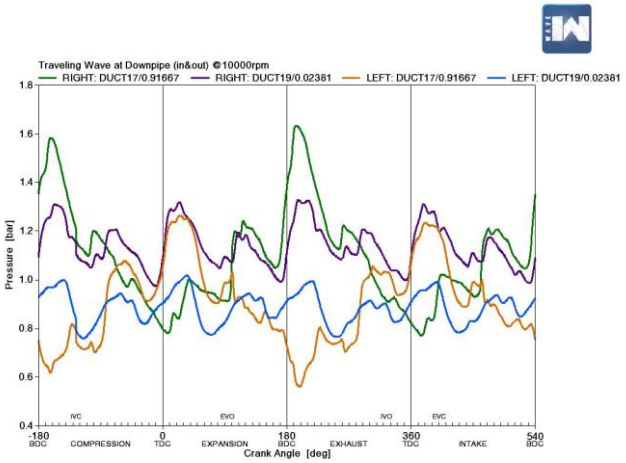

Pressure plot of downpipe - Fig 7.3

Moreover, the development of secondary collector established downpipe's internal diameter equal to 44.45mm, as the parameter influences the collector's acoustic impedance and hence the extent of wave reflection and transmission.

The downpipe was designed with a 90° bend with bend radius of 3 x Pipe OD, to change the direction of exhaust gas, without creating possibilities of pressure loss due to flow separation. Apart from this, the smooth transition allows accurate and predictable engine exhaust and muffler acoustic analysis, like those performed on the muffler only, to predict transmission loss vs frequency characteristics.

Modified exhaust manifold with collector extension was meshed using WaveMesher (Fig 7.4(i)) and imported to the engine model on Wave (Fig 7.4 (ii)) to evaluate the results of its presence on total exhaust performance and efficiency based on its assistance offered for exhaust scavenging and variations in volumetric efficiency (Fig 7.5 (i, ii & iii)).

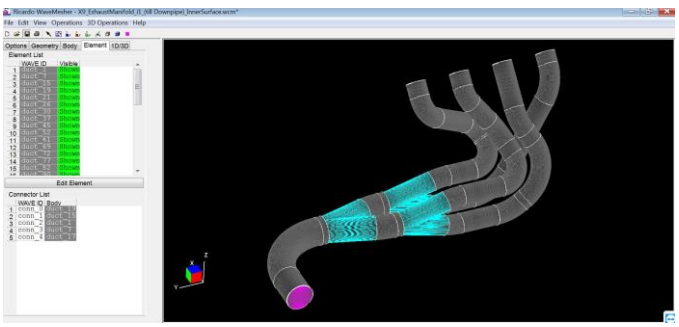

Exhaust system meshed on Ricardo WaveMesher - Fig 7.4 (i)

International Journal of Scientific & Engineering Research, Volume 9, Issue 10, October-2018
ISSN 2229-5518

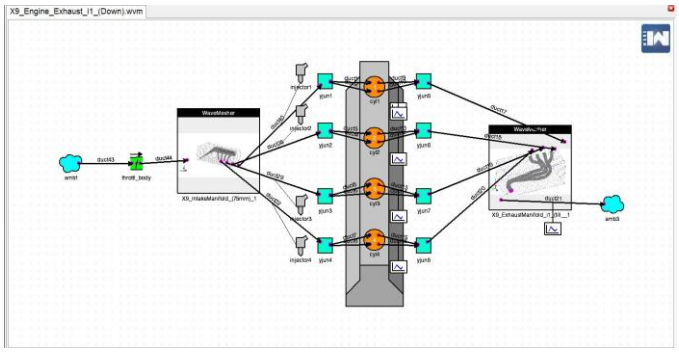

Engine theoretical model on Ricardo WaveBuild - Fig 7.4 (ii)

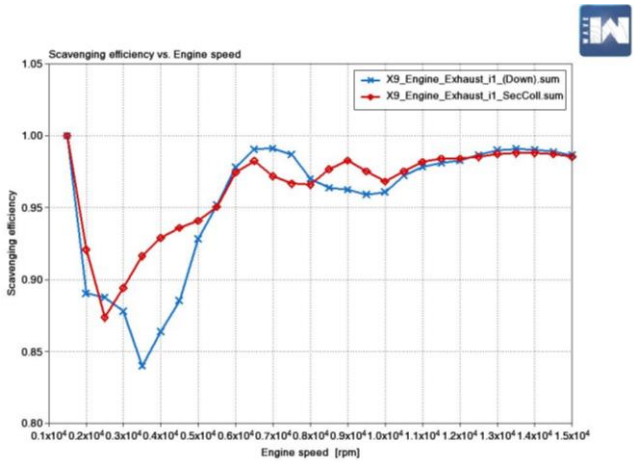

Exhaust scavenging efficiency – comparing exhaust with and without collector extension - Fig 7.5 (i)

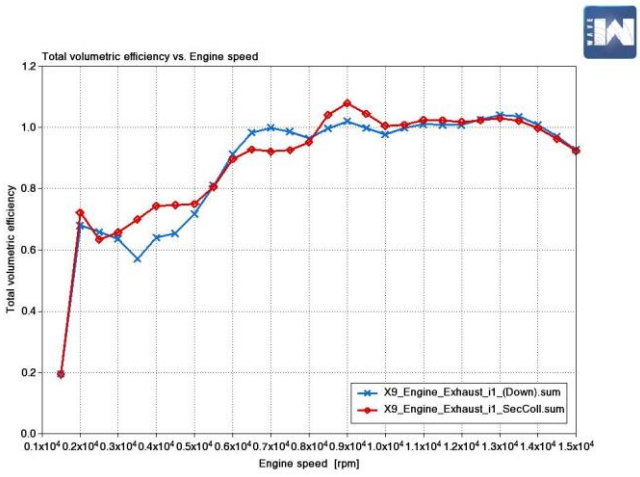

Volumetric efficiency – comparing exhaust with and without collector extension -Fig 7.5 (ii)

8 Exhaust Manifold Design Optimization

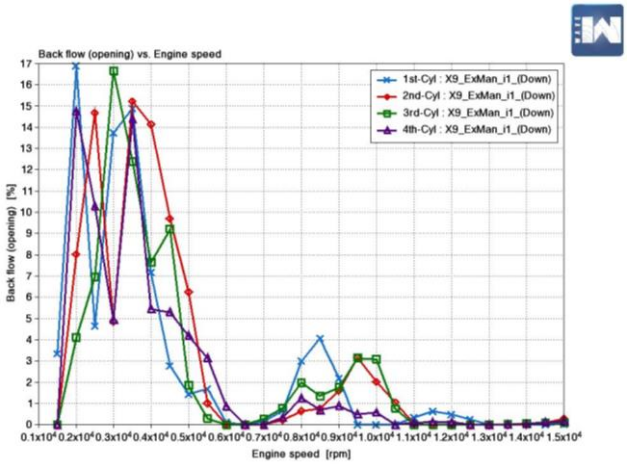

Exhaust gas backflow (at intake valve opening) – Fig 8.1

(Fig 8.1) above, shows the percentage of exhaust gas backflow tendency, at intake valve opening, for all four cylinders indicating the uniformity of exhaust scavenging and intake charge delivery. These plots were studied to optimize the characteristics of exhaust gas flow in all primary headers in order to maintain uniformity amongst all cylinders. The bend positions with respect to exhaust port location and number of bends were varied, keeping the effective primary header length constant and close to the optimum calculated value. Moreover, ease in manufacturing of bends and fixture for welding was also considered while making these variations.

It was observed from the data from these graphs that increasing the location of bends in the primary header further from the exhaust port improves gas flow due to lesser tendency of flow separation hence delivering higher gas velocities and better scavenging.

The final iteration was designed showing low rpm exhaust gas back flow characteristics reduced from a range of 5,500 (Fig 9.1) to 4,500 rpm (Fig 8.2 (i)), with almost same peak amplitude of theoretical back flow percentage of 17%. Moreover, the headers were modified to deliver total volumetric efficiency in each cylinder with under $\pm$ 5% deviation at high rpm engine operation (Fig 8.2(ii)) and with equivalent VE at lower rpms.

International Journal of Scientific & Engineering Research, Volume 9, Issue 10, October-2018
ISSN 2229-5518

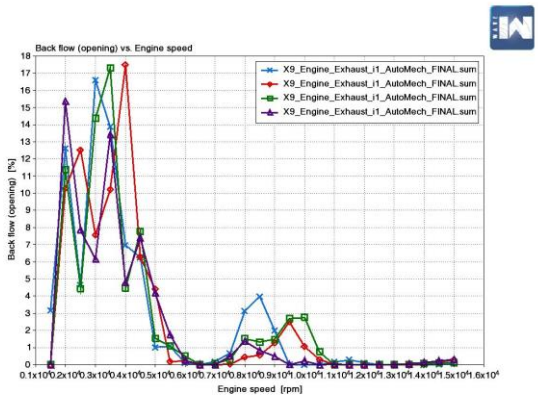

Exhaust back flow percentage – comparing all four cylinders – Fig 8.2 (i)

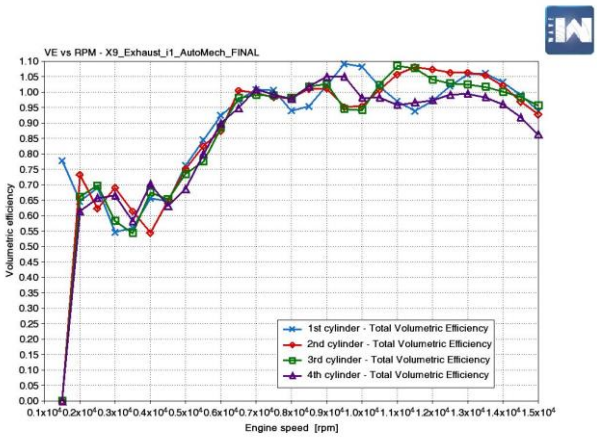

Total volumetric efficiency in each of the four cylinders – Fig 8.2 (ii)

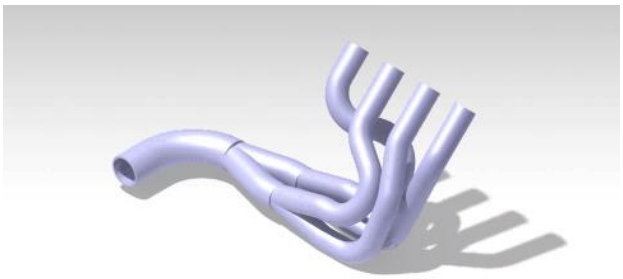

Fig 8.3 (i)

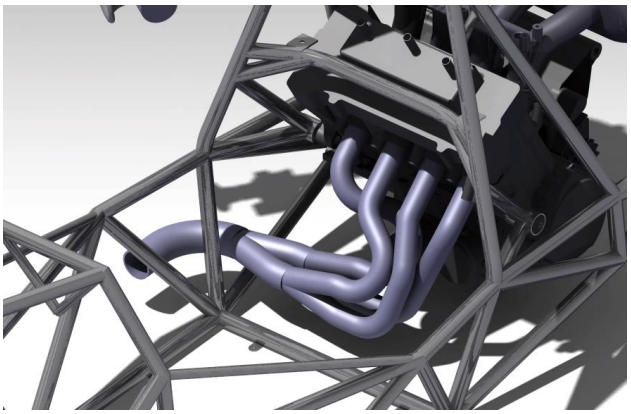

Exhaust manifold render showing its orientation with respect to the engine and chassis - Fig 8.3 (ii)

9 Results

9.1 Engine Performance Comparison Between Previous & Newly Developed Exhaust Manifold Designs

The fine tuned exhaust manifold concurs with the predicted peak torque rpm, reaching the pinnacle of 53 Nm at 9,500 rpm. 5.35% peak torque was compromsed to achieve a flat torque curve from 7,000 rpm till 12,000 rpm (Fig 9.a(i)). Moreover, an average volumetric efficiency between all cylinders was also maintained at 100% continuously after 7,000 rpm through trading-off 6.8% maximum value from previous engine model (Fig 9.a(ii)). 17.68% improvement in scavenging efficiency at lower rpms was also observered (Fig 9.a(iii)). Conclusivly, more linear and tractable power characteristics was obtained, reaching a maximum of 88 bhp at 14,000 rpm (Fig 9.a(iv)).

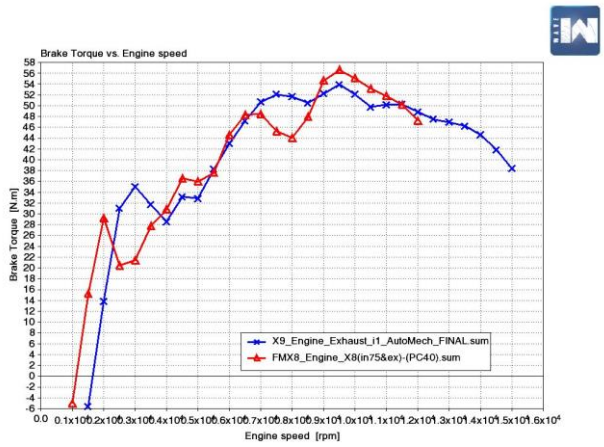

Fig 9.a(i)

International Journal of Scientific & Engineering Research, Volume 9, Issue 10, October-2018
ISSN 2229-5518

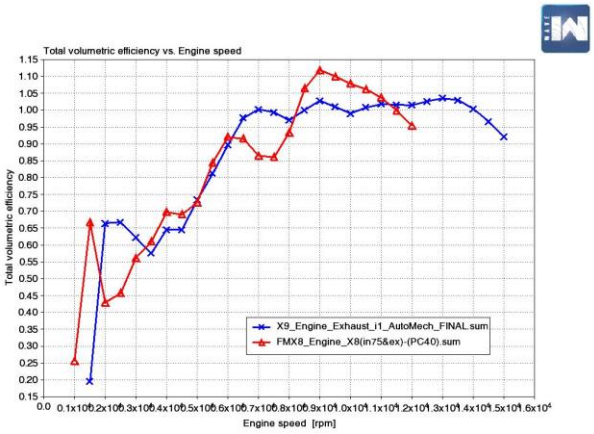

Fig 9.a(ii)

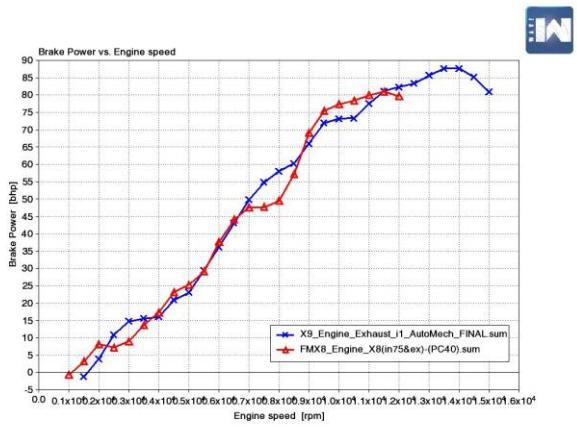

Fig 9.a(iv)

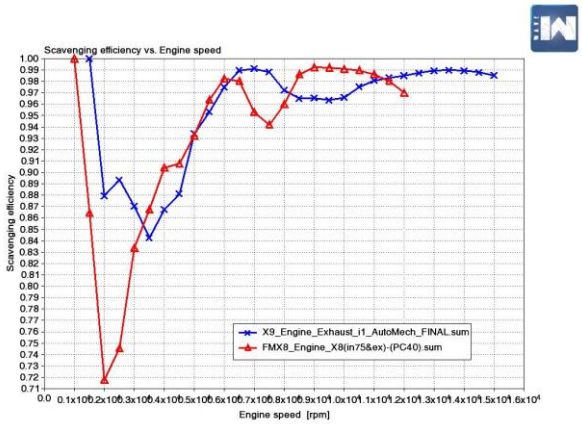

Fig 9.a(iii)

Primary Header Length Calculations:	Crank RPM	Cam RPM	Real Time Required for 1deg Cam Revolution	Real Time Required for 2S.3deg Cam Revolution	Length of Header (1st Harmonic)	1 Harmonic length (mm)	Length of Header (2nd Harmonic)	2 Harmonic length (mm)	Length of Header (3rd Harmonic)	3 Harmonic length (mm)
	1000	500	0.000333333	0.084333333	28.75197793	2863.97793	14.37598897	14135.98897	7.187994483	6827.99448
	1500	750	0.000222222	0.056222222	19.16798529	19047.98529	9.583992644	9343.992644	4.791996322	4431.99632
	2000	1000	0.000166667	0.042166667	14.37598897	14255.98897	7.187994483	6947.994483	3.593997241	3233.99724
	2500	1250	0.000133333	0.033733333	11.50079117	11380.79117	5.750395586	5510.395586	2.875197793	2515.19779
	3000	1500	0.000111111	0.02811111	9.583992644	9463.992644	4.791996322	4551.996322	2.395998161	2035.99816
	3500	1750	9.52381E-05	0.024095238	8.214850838	8094.850838	4.107425419	3867.425419	2.053712709	1693.71271
	4000	2000	8.33333E-05	0.021083333	7.187994483	7067.994483	3.593997241	3353.997241	1.796998621	1436.99862
	4500	2250	7.40741E-05	0.018740741	6.389328429	6269.328429	3.194664215	2954.664215	1.597332107	1237.33211
	5000	2500	6.66667E-05	0.016866667	5.750395586	5630.395586	2.875197793	2635.197793	1.437598897	1077.5989
	5500	2750	6.06061E-05	0.015333333	5.227632351	5107.632351	2.613816176	2373.816176	1.306908088	946.908088
	6000	3000	5.55556E-05	0.014055556	4.791996322	4671.996322	2.395998161	2155.998161	1.19799908	837.99908
	6500	3250	5.12821E-05	0.012974359	4.42338122	4303.38122	2.21169061	1971.69061	1.105845305	745.845305
	7000	3500	4.7619E-05	0.012047619	4.107425419	3987.425419	2.053712709	1813.712709	1.026856355	666.856355
	7500	3750	4.44444E-05	0.011244444	3.833597058	3713.597058	1.916798529	1676.798529	0.958399264	598.399264
	8000	4000	4.16667E-05	0.010541667	3.593997241	3473.997241	1.796998621	1556.998621	0.89849931	538.49931
	8500	4250	3.92157E-05	0.009921569	3.382585639	3262.585639	1.69129282	1451.29282	0.84564641	485.64641
	9000	4500	3.7037E-05	0.00937037	3.194664215	3074.664215	1.597332107	1357.332107	0.798666054	438.666054
	9500	4750	3.50877E-05	0.008877193	3.026523993	2906.523993	1.513261996	1273.261996	0.756630998	**396.631**
	9750	4875	3.4188E-05	0.008649573	2.948920814	2828.920814	1.474460407	1234.460407	0.737230203	**377.2302**
	10000	5000	3.33333E-05	0.008433333	2.875197793	2755.197793	1.437598897	1197.598897	0.718799448	**358.7994**
	10500	5250	3.1746E-05	0.008031746	2.738283613	2618.283613	1.369141806	1129.141806	0.684570903	324.570903
	11000	5500	3.0303E-05	0.007666667	2.613816176	2493.816176	1.306908088	1066.908088	0.653454044	293.454044
	11500	5750	2.89855E-05	0.007333333	2.500171994	2380.171994	1.250085997	1010.085997	0.625042999	265.042999
	12000	6000	2.77778E-05	0.007027778	2.395998161	2275.998161	1.19799908	957.9990805	0.59899954	238.99954
	12500	6250	2.66667E-05	0.006746667	2.300158235	2180.158235	1.150079117	910.0791173	0.575039559	215.039559
	13000	6500	2.5641E-05	0.006487179	2.21169061	2091.69061	1.105845305	865.8453051	0.552922653	192.922653
	13500	6750	2.46914E-05	0.006246914	2.129776143	2009.776143	1.064888072	824.8880716	0.532444036	172.444036
	14000	7000	2.38095E-05	0.00602381	2.053712709	1933.712709	1.026856355	786.8563547	0.513428177	153.428177
	14500	7250	2.29885E-05	0.005816092	1.98289503	1862.89503	0.991447515	751.4475149	0.495723757	135.723757
	15000	7500	2.22222E-05	0.005622222	1.916798529	1796.798529	0.958399264	718.3992644	0.479199632	119.199632

Primary Header Effective Length Calculation – Fig 4.4

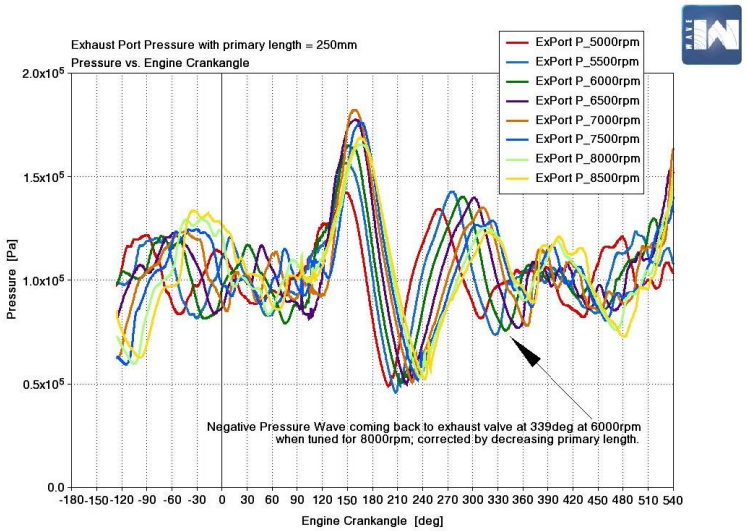

Fig 4.10

Secondary Header Length Calculations:	Crank RPM	Cam RPM	Real Time Required for 1deg Cam Revolution	Real Time Required for (360)deg Cam Revolution	Length of Secondary (1st Harmonic)	Length of Secondary (2nd Harmonic)	Length of Secondary (3rd Harmonic)	Length of Secondary (4th Harmonic)	(4th)Predicted primary length after deducing correction & part	Length of Secondary (5th Harmonic)	(5th)Predicted primary length after deducing correction & part
	1000	500	0.000333333	0.06	17.71537468	8.857687339	4.42884367	2.214421835	2214.421835	1.107210917	1107.210917
	1500	750	0.000222222	0.04	11.81024979	5.905124893	2.952562446	1.476281223	1476.281223	0.738140612	738.1406116
	2000	1000	0.000166667	0.03	8.857687339	4.42884367	2.214421835	1.107210917	1107.210917	0.553605459	553.6054587
	2500	1250	0.000133333	0.024	7.086149871	3.543074936	1.771537468	0.885768734	885.7687339	0.442884367	442.884367
	3000	1500	0.00011111	0.02	5.905124893	2.952562446	1.476281223	0.738140612	738.1406116	0.369070306	369.0703058
	3500	1750	9.52381E-05	0.017142857	5.061535622	2.530767811	1.265383906	0.632691953	632.6919528	0.316345976	316.3459764
	4000	2000	8.33333E-05	0.015	4.42884367	2.214421835	1.107210917	0.553605459	553.6054587	0.276802729	276.8027294
	4500	2250	7.40741E-05	0.013333333	3.936749929	1.968374964	0.984187482	0.492093741	492.0937411	0.246046871	246.0468705
	5000	2500	6.66667E-05	0.012	3.543074936	1.771537468	0.885768734	0.442884367	442.884367	0.221442183	221.4421835
	5500	2750	6.06061E-05	0.010909091	3.220977214	1.610488607	0.805244304	0.402622152	402.6221518	0.201311076	201.3110759
	6000	3000	5.55556E-05	0.01	2.952562446	1.476281223	0.738140612	0.369070306	369.0703058	0.184535153	184.5351529
	6500	3250	5.12821E-05	0.009230769	2.725442258	1.362721129	0.681360565	0.340680282	340.6802823	0.170340141	170.3401411
	7000	3500	4.7619E-05	0.008571429	2.530767811	1.265383906	0.632691953	0.316345976	316.3459764	0.158172988	158.1729882
	7500	3750	4.44444E-05	0.008	2.362049957	1.181024979	0.590512489	0.295256245	295.2562446	0.147628122	147.6281223
	8000	4000	4.16667E-05	0.0075	2.214421835	1.107210917	0.553605459	0.276802729	276.8027294	0.138401365	138.4013647
	8500	4250	3.92157E-05	0.007058824	2.084161727	1.042080863	0.521040432	0.260520216	260.5202159	0.130260108	130.2601079
	9000	4500	3.7037E-05	0.006666667	1.968374964	0.984187482	0.492093741	0.246046871	246.0468705	0.123023435	123.0234353
	9500	4750	3.50877E-05	0.006315789	1.864776282	0.932388141	0.46619407	0.233097035	233.0970352	0.116548518	116.5485176
	10000	5000	3.33333E-05	0.006	1.771537468	0.885768734	0.442884367	0.221442183	221.4421835	0.110721092	**110.7210917**
	10500	5250	3.1746E-05	0.005714286	1.687178541	0.84358927	0.421794635	0.210897318	210.8973176	0.105448659	105.4486588
	11000	5500	3.0303E-05	0.005454545	1.610488607	0.805244304	0.402622152	0.201311076	201.3110759	0.100655538	100.6555379
	11500	5750	2.89855E-05	0.005217391	1.540467363	0.770233682	0.385116841	0.19255842	192.5584204	0.09627921	96.27921021
	12000	6000	2.77778E-05	0.005	1.476281223	0.738140612	0.369070306	0.184535153	184.5351529	0.092267576	92.26757645
	12500	6250	2.66667E-05	0.0048	1.417229974	0.708614987	0.354307494	0.177153747	177.1537468	0.088576873	88.57687339
	13000	6500	2.5641E-05	0.004615385	1.362721129	0.681360565	0.340680282	0.170340141	170.3401411	0.085170071	85.17007057
	13500	6750	2.46914E-05	0.004444444	1.312249976	0.656124988	0.328062494	0.164031247	164.031247	0.082015624	82.01562351
	14000	7000	2.38095E-05	0.004285714	1.265383906	0.632691953	0.316345976	0.158172988	158.1729882	0.079086494	79.0864941
	14500	7250	2.29885E-05	0.004137931	1.221749978	0.610874989	0.305437494	0.152718747	152.7187472	0.076359374	76.35937361
	15000	7500	2.22222E-05	0.004	1.181024979	0.590512489	0.295256245	0.147628122	147.6281223	0.073814061	73.81406116

Secondary Header Effective Length Calculation – Fig 6.2

Downpipe Length Calculations:	Crank RPM	Cam RPM	Real Time Required for 1deg Cam Revolution	Real Time Required for (360)deg Cam Revolution	Length of Secondary (1st Harmonic)	Length of Secondary (2nd Harmonic)	Length of Secondary (3rd Harmonic)	Length of Secondary (4th Harmonic)	(4th)Predicted primary length after deducing correction & part	Length of Secondary (5th Harmonic)	(5th)Predicted primary length after deducing correction & part	Length of Secondary (6th Harmonic)	(6th)Predicted primary length after deducing correction & part
	1000	500	0.000333333	0.12	33.40443084	16.70221542	8.351107711	4.175553855	4175.553855	2.087776928	2087.776928	1.043888464	1043.888464
	1500	750	0.000222222	0.08	22.26962056	11.13481028	5.567405141	2.78370257	2783.70257	1.391851285	1391.851285	0.695925643	695.9256426
	2000	1000	0.000166667	0.06	16.70221542	8.351107711	4.175553855	2.087776928	2087.776928	1.043888464	1043.888464	0.521944232	521.9442319
	2500	1250	0.000133333	0.048	13.36177234	6.680886169	3.340443084	1.670221542	1670.221542	0.835110771	835.1107711	0.417555386	417.5553855
	3000	1500	0.000111111	0.04	11.13481028	5.567405141	2.78370257	1.391851285	1391.851285	0.695925643	695.9256426	0.347962821	347.9628213
	3500	1750	9.52381E-05	0.034285714	9.544123098	4.772061549	2.386030775	1.193015387	1193.015387	0.596507694	596.5076936	0.298253847	298.2538468
	4000	2000	8.33333E-05	0.03	8.351107711	4.175553855	2.087776928	1.043888464	1043.888464	0.521944232	521.9442319	0.260972116	260.972116
	4500	2250	7.40741E-05	0.026666667	7.423206854	3.711603427	1.855801714	0.927900857	927.9008568	0.463950428	463.9504284	0.231975214	231.9752142
	5000	2500	6.66667E-05	0.024	6.680886169	3.340443084	1.670221542	0.835110771	835.1107711	0.417555386	417.5553855	0.208777693	208.7776928
	5500	2750	6.06061E-05	0.021818182	6.073532881	3.03676644	1.51838322	0.75919161	759.1916101	0.379595805	379.595805	0.189797903	189.7979025
	6000	3000	5.55556E-05	0.02	5.567405141	2.78370257	1.391851285	0.695925643	695.9256426	0.347962821	347.9628213	0.173981411	173.9814106
	6500	3250	5.12821E-05	0.018461538	5.139143207	2.569571603	1.284785802	0.642392901	642.3929008	0.32119645	321.1964504	0.160598225	160.5982252
	7000	3500	4.7619E-05	0.017142857	4.772061549	2.386030775	1.193015387	0.596507694	596.5076936	0.298253847	298.2538468	0.149126923	149.1269234
	7500	3750	4.44444E-05	0.016	4.453924113	2.226962056	1.113481028	0.556740514	556.7405141	0.278370257	278.370257	0.139185129	139.1851285
	8000	4000	4.16667E-05	0.015	4.175553855	2.087776928	1.043888464	0.521944232	521.9442319	0.260972116	260.972116	0.130486058	130.486058
	8500	4250	3.92157E-05	0.014117647	3.92993304	1.96496652	0.98248326	0.49124163	491.2416301	0.245620815	245.620815	0.122810408	122.8104075
	9000	4500	3.7037E-05	0.013333333	3.711603427	1.855801714	0.927900857	0.463950428	463.9504284	0.231975214	231.9752142	0.115987607	115.9876071
	9500	4750	3.50877E-05	0.012631579	3.516255878	1.758127939	0.87906397	0.439531985	439.5319848	0.219765992	219.7659924	0.109882996	109.8829962
	10000	5000	3.33333E-05	0.012	3.340443084	1.670221542	0.835110771	0.417555386	417.5553855	0.208777693	**208.7776928**	0.104388846	104.3888464
	10500	5250	3.1746E-05	0.011428571	3.181374366	1.590687183	0.795343592	0.397671796	397.6717958	0.198835898	198.8358979	0.099417949	99.41794894
	11000	5500	3.0303E-05	0.010909091	3.03676644	1.51838322	0.75919161	0.379595805	379.595805	0.189797903	189.7979025	0.094898951	94.89895126
	11500	5750	2.89855E-05	0.010434783	2.904733117	1.452366558	0.726183279	0.36309164	363.0916396	0.18154582	181.5458198	0.09077291	90.7729099
	12000	6000	2.77778E-05	0.01	2.78370257	1.391851285	0.695925643	0.347962821	347.9628213	0.173981411	173.9814106	0.086990705	86.99070532
	12500	6250	2.66667E-05	0.0096	2.672354468	1.336177234	0.668088617	0.334044308	334.0443084	0.167022154	167.0221542	0.083511077	83.51107711
	13000	6500	2.5641E-05	0.009230769	2.569571603	1.284785802	0.642392901	0.32119645	321.1964504	0.160598225	160.5982252	0.08029913	80.29911261
	13500	6750	2.46914E-05	0.008888889	2.474402285	1.237201142	0.618600571	0.309300286	309.3002856	0.154650143	154.6501428	0.077325071	77.3250714
	14000	7000	2.38095E-05	0.008571429	2.386030775	1.193015387	0.596507694	0.298253847	298.2538468	0.149126923	149.1269234	0.074563462	74.5634617
	14500	7250	2.29885E-05	0.008275862	2.303753851	1.151876926	0.575938463	0.287969231	287.9692314	0.143984616	143.9846157	0.071992308	71.99230785
	15000	7500	2.22222E-05	0.008	2.226962056	1.113481028	0.556740514	0.278370257	278.370257	0.139185129	139.1851285	0.069592564	69.59256426

Downpipe or Collector Extension Effective Length Calculation – Fig 7.2

International Journal of Scientific & Engineering Research, Volume 9, Issue 10, October-2018
ISSN 2229-5518

10 REFERENCES

[1] Exhaust Science Demystified (http://www.superchevy.com/how-to/exhaust/0505phr-exh/)
[2] A New Simple Friction Model for S. I. Engine - Emiliano Pipitone (SAE Technical Paper, 2009-01-1984)
[3] Nature of Heat Release Rate in an Engine - IITD (web.iitd.ac.in/~pmvs/courses/mel713/mel713-20.ppt)
[4] Willard. W. Pulkrabeck (engineering-fundamentals-of-the-internal-combustion-engine)
[5] Open and Closed Organ Pipes (https://newt.phys.unsw.edu.au/jw/flutes.v.clarinets.html)
[6] Pipes and Harmonics (https://newt.phys.unsw.edu.au/jw/pipes.html)
[7] Difference between shorty and full length headers (http://garage.grumpysperformance.com/index.php?threads/differance-between-shorty-and-full-length-headers.1303/)
[8] Jack Burns – The Sultan of Stainless (https://www.hotrod.com/articles/0310phr-jack-burns-exhaust-manifold-header-tech/)
[9] Exhaust System Technology (http://www.epi-eng.com/piston_engine_technology/exhaust_system_technology.htm)